

Ab initio calculations of two-electron emission by attosecond pulses

J. Feist¹, R. Pazourek¹, S. Nagele¹, E. Persson¹, B. I. Schneider^{2,3},
L. A. Collins⁴, and J. Burgdörfer¹

¹ Institute for Theoretical Physics, Vienna University of Technology, 1040 Vienna, Austria, EU

² Physics Division, National Science Foundation, Arlington, Virginia 22230, USA

³ Electron and Atomic Physics Division, National Institute of Standards and Technology, Gaithersburg, Maryland 20899, USA

⁴ Theoretical Division, Los Alamos National Laboratory, Los Alamos, New Mexico 87545, USA

E-mail: johannes.feist@tuwien.ac.at

Abstract. Recent experimental developments of high-intensity, short-pulse XUV light sources are enhancing our ability to study electron-electron correlations. We perform time-dependent calculations to investigate the so-called “sequential” regime ($\hbar\omega > 54.4$ eV) in the two-photon double ionization of helium. We show that attosecond pulses allow to not only probe but also to induce angular and energy correlations of the emitted electrons. Electron correlation induced by the time correlation between emission events manifests itself in the angular distribution of the ejected electrons. The final momentum distribution reveals regions dominated by the Wannier ridge break-up scenario and by post-collision interaction. In addition, we find evidence for an interference between direct (“nonsequential”) and indirect (“sequential”) double photo-ionization with intermediate shake-up states, the strength of which is controlled by the pulse duration.

1. Introduction

Understanding the role of electron correlation in atoms, molecules, and solids has been a central theme in physics and chemistry since the early days of quantum mechanics. Most of the focus has centered on the role of electron correlation in (quasi-)stationary states. The recent progress in the development of ultrashort and intense light sources [1–10] provides unprecedented opportunities to study the effects of correlation not only in stationary states, but also in transient states, and even to actively induce dynamical correlations.

The simplest system where electron-electron interaction can be studied is the helium atom, with its double ionization being the prototype reaction for a three-body Coulomb breakup. Unraveling the intricacies of electron correlation in ultrashort and intense electromagnetic fields interacting with this simple atom is critical to our understanding of the same processes in more complex systems. While computationally challenging, the full dynamics of the helium atom can still be accurately simulated in *ab initio* calculations [11]. With the advent of intense XUV pulses, the focus has shifted from single-photon double ionization [12–16] and intense-IR laser ionization by rescattering [17–19] to multiphoton ionization. Two-photon double ionization (TPDI) has recently received considerable attention, both in the so-called “nonsequential” or “direct” regime (39.5 eV $< \hbar\omega < 54.4$ eV), where the electrons necessarily have to share energy via electron-electron

interaction to achieve double ionization [20–33], and in the “sequential” regime ($\hbar\omega > 54.4$ eV), where electron-electron interaction is not a priori necessary [34–42].

We perform *ab initio* simulations of the interaction of ultrashort laser pulses with a helium atom (cf. [29]). We present our recent results on two-photon double ionization of He by ultrashort pulses for photon energies above the ionization potential of the He⁺ ground state. Double ionization in this regime proceeds in two steps: single ionization of He followed by ionization of the remaining He⁺ ion. By using attosecond XUV pulses, these two separated stages of the sequential process can be confined to within a short time interval of each other. For an ultrashort pulse of attosecond duration the concept of “sequential interactions”, valid for long pulses, becomes meaningless [35–37, 39]. Instead, the two-electron emission occurs almost simultaneously, and the strength of electron correlation in the exit channel can be tuned by the pulse duration T . We show that this can be used to not only probe, but actively induce correlations between the electrons [42]. We can then make connections to well-known scenarios of collision physics, such as the Wannier ridge breakup mode and post-collision interaction. In longer pulses of a few femtoseconds duration, a novel interference effect between the sequential channel associated with shake-up of the intermediate ion and the nonsequential channel without shake-up appears [41]. This interference, which produces Fano-like resonances, is controlled by the duration of the pulse, providing a possible route towards measuring the duration of X-ray free-electron laser (XFEL) pulses.

All this information is encoded in the final joint momentum distribution $P^{DI}(\mathbf{k}_1, \mathbf{k}_2) \equiv P^{DI}(E_1, E_2, \Omega_1, \Omega_2)$, which is experimentally accessible in kinematically complete cold-target recoil-ion-momentum spectroscopy (COLTRIMS) measurements [43]. Unless otherwise stated, atomic units are used.

2. Method

As in our previous paper [29], we solve the time-dependent Schrödinger equation in its full dimensionality, including all inter-particle interactions. The laser field is linearly polarized and treated in dipole approximation, with the vector potential

$$A(t) = A_0 \cos(\omega t) \begin{cases} \sin^2(\pi t/T) & 0 < t < T \\ 0 & \text{otherwise} \end{cases}, \quad (1)$$

where ω is the mean frequency of the field, and A_0 is the peak value for the vector potential. This is chosen such that the peak intensity of the laser field is $I_0 = 10^{12}$ W/cm². In this regime, depletion of ground and intermediate states is negligible. We checked that using $I_0 = 5 \cdot 10^{15}$ W/cm² does not strongly influence the results even for the longest pulse ($T = 9$ fs). T is the *total* duration of the pulse. The FWHM of the field is $T/2$, while the FWHM of the *intensity envelope*, which is commonly used to characterize the duration of ultrashort pulses, is approximately a third of the total duration T .

The computational approach is based on a time-dependent close-coupling (TDCC) scheme where the angular variables are expanded in coupled spherical harmonics (using single electron angular momenta up to $l_{\max} = 10$ and a total angular momentum up to $L_{\max} = 3$). The two radial variables are discretized via a finite element discrete variable representation (FEDVR) (with box sizes up to 800 a.u.). Temporal propagation is performed by the short iterative Lanczos (SIL) algorithm with adaptive time-step control, starting from the ground state. The asymptotic momentum distribution is obtained by projecting the wave packet onto products of Coulomb continuum states. Projection errors due to the replacement of the full three-body final state by independent-particle Coulomb wave functions can be reduced to the one-percent level by delaying the time of projection until the two electrons are sufficiently far apart from each other [29]. All results were checked for numerical convergence.

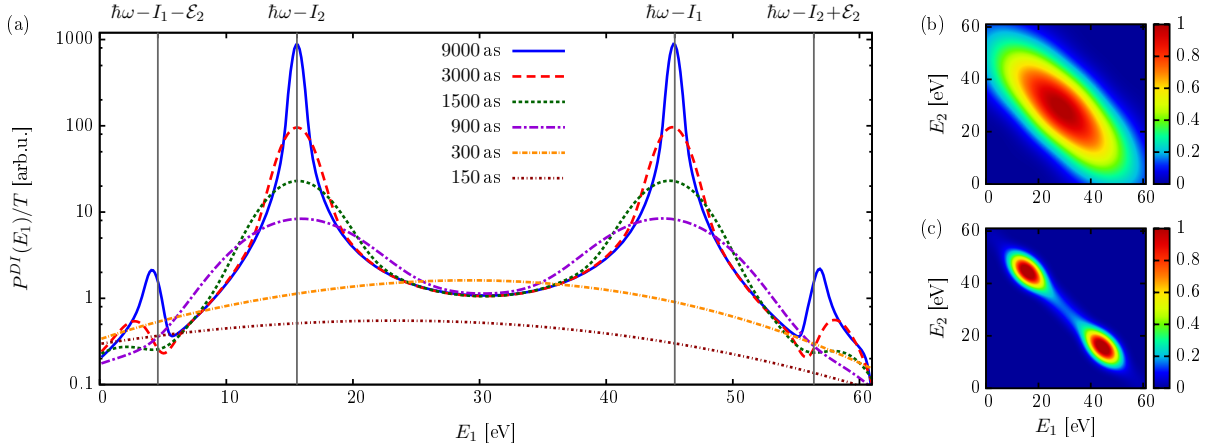


Figure 1: (a) Double ionization (DI) rate $P^{DI}(E)/T$ (i.e. DI probability divided by the pulse duration) for TPDI by an XUV pulse at $\hbar\omega = 70$ eV with different pulse durations T . For sufficient pulse duration, the DI rate converges to a stable value except near the peaks of the sequential process. (b) and (c) show the two-electron energy spectrum $P^{DI}(E_1, E_2)$ for (b) $T = 300$ as and (c) $T = 900$ as.

3. TPDI by ultrashort pulses

The (joint) energy probability distribution (previously investigated in [35–37, 39])

$$P^{DI}(E_1, E_2) = \iint P^{DI}(E_1, E_2, \Omega_1, \Omega_2) d\Omega_1 d\Omega_2 \quad (2)$$

reveals the breakdown of the sequential ionization picture with decreasing pulse duration T (Figure 1). For long pulses, two distinct peaks signifying the emission of the “first” electron with energy $E_1 = \hbar\omega - I_1$ (with the first ionization potential $I_1 = 24.6$ eV) and the “second” electron with $E_2 = \hbar\omega - I_2$ ($I_2 = 54.4$ eV) are clearly visible.

For pulses of the order of one hundred attoseconds, a dramatically different picture emerges: the two peaks merge into a single one located near the point of symmetric energy sharing. This effect is not simply due to the Fourier broadening of the pulse (cf. [39]), which determines the uncertainty in the total energy E_{tot} (i.e. the width along lines with $E_1 - E_2 = \text{const}$). Instead, the close proximity in time of the two emission events causes the energy of the intermediate state to be ill-defined, representing a clear departure from the independent-particle behavior. Differently stated, the time interval between the two ionization events is too short for the remaining He^+ ion to relax to a stationary state before the second electron is ejected. This demonstrates that in the limit of ultrashort pulses, the distinction between “sequential” and “nonsequential” ionization loses its significance. Although electron interaction is not necessary to achieve double ionization, it has a significant effect on the outgoing electrons. This has been called the “transient” regime previously [39], and is entered when the duration of the XUV pulse is comparable to the “correlation time” defined by $T_C = 2\pi/E_C \approx 139$ as, where $E_C = I_2 - I_1$ is the energy difference between the two ionization potentials.

The attosecond-pulse induced dynamical electron correlation becomes more clearly visible in the joint angular distribution $P^{DI}(\theta_1, \theta_2)$ (Figure 2a), where θ_1 and θ_2 are the polar emission angles of the electrons with respect to the polarization axis of the XUV pulse, and the energies E_1, E_2 are integrated over. Here and in the following we choose coplanar geometry (azimuthal angles $\phi_1 = \phi_2 = 0^\circ$). Calculations in non-coplanar geometry lead to the same conclusions. In the limit of “long” pulses ($T = 9$ fs), the joint angular distribution approaches the product of two

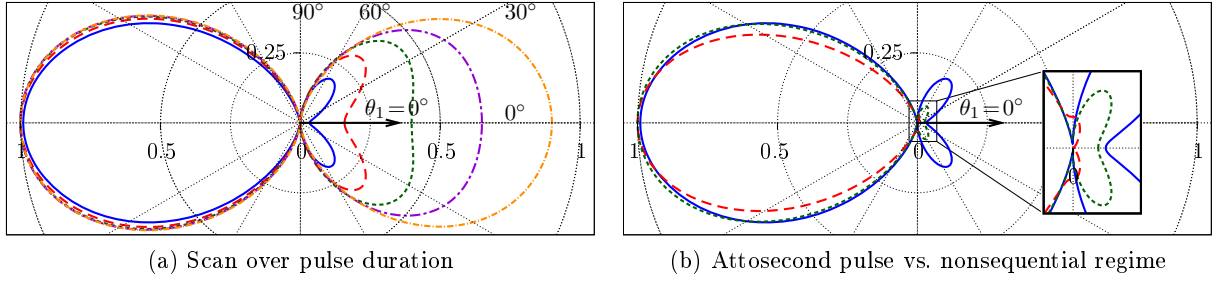


Figure 2: Conditional angular distributions $P^{DI}(\theta_1 = 0^\circ, \theta_2)$ for TPDI with \sin^2 pulses. For better comparison the distributions are normalized to a maximum value of one at $P^{DI}(\theta_1 = 0^\circ, \theta_2 = 180^\circ)$. In (a), the pulse duration in the sequential regime ($\hbar\omega = 70$ eV) is varied. Long pulses $T \geq 3$ fs show independent dipolar distributions for the two electrons, whereas attosecond pulses lead to a strong preference for back-to-back emission. The durations (from outside to inside) are $T = 9000$ as, 1500 as, 600 as, 300 as, and 150 as (solid blue). (b) compares an ultrashort pulse ($T = 150$ as) at $\hbar\omega = 70$ eV (solid blue) with “long” ($T = 4$ fs) pulses in the nonsequential regime (42 eV, dashed red, and 52 eV, dash-dotted green). The distribution for the ultrashort pulse strongly resembles the long-pulse distribution in the nonsequential regime.

independent Hertz dipoles, each of which signifies the independent interaction of one electron with one photon. Consequently, also the conditional angular distribution $P^{DI}(\theta_1 = 0^\circ, \theta_2)$ corresponds to a Hertz dipole. With decreasing pulse duration, $P^{DI}(\theta_1 = 0^\circ, \theta_2)$ is strongly modified and develops a pronounced forward-backward asymmetry (Figure 2a). The conditional probability for the second electron to be emitted in the same direction as the first is strongly suppressed. This strong preference for back-to-back emission for $T \leq 300$ as persists after integration over the electron energies, i.e. it does not only occur for some specific choice of energy sharing. Nevertheless, approximately equal energy sharing dominates (cf. Figure 1). Thus, the dominant break-up mode induced by an attosecond pulse corresponds to the “Wannier ridge” configuration [44]. This resembles the nonsequential TPDI regime ($\hbar\omega < 54.4$ eV, cf. [29]), where only back-to-back configurations are observed as well (Figure 2b). Here the electrons need to exchange energy to achieve double ionization, so that even in long pulses only electrons ionized within a short time of each other can be observed.

One remarkable feature of the conditional angular distribution is the persistence of the nodal plane at $\theta = 90^\circ$. While correlation effects strongly perturb the shape of the independent-particle dipolar shape, the nodal plane, expected for the angular distribution of two electrons absorbing one photon each, is preserved almost completely. Note that this also holds true in the nonsequential TPDI regime for energies approaching the sequential threshold (cf. [29]). This is in contrast to one-photon double ionization, where only one electron absorbs the photon energy and electron ejection at angles normal to the polarization axis is indeed observed [14].

To better quantify the amount of correlation between the electrons, we examine the *mutual information* [45] contained within their joint angular distribution. In essence, mutual information measures the information that the two variables share – i.e. how much information one gains about the second variable by knowing the first. For the angular variables, it is defined by

$$\mathcal{I}_{\Omega_1, \Omega_2} = \iint d\Omega_1 d\Omega_2 P_n^{DI}(\Omega_1, \Omega_2) \log_2 \left(\frac{P_n^{DI}(\Omega_1, \Omega_2)}{P_n^{DI}(\Omega_1) P_n^{DI}(\Omega_2)} \right), \quad (3)$$

where $P_n^{DI}(\Omega_1)$ and $P_n^{DI}(\Omega_2)$ are the normalized reduced one-variable distributions. If the two variables are independent, the mutual information vanishes. The mutual information is

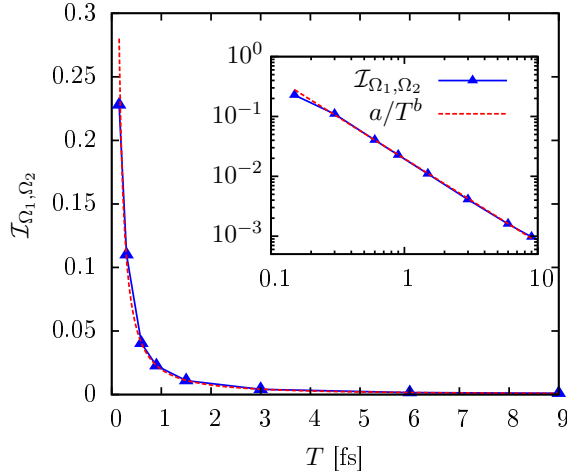


Figure 3: Mutual information $\mathcal{I}_{\Omega_1, \Omega_2}$ after TPDI at $\hbar\omega = 70$ eV, for \sin^2 pulses of different total duration T . The inset shows the same data using a log-log scale. The fit shows that the mutual information follows a power law dependence, with $b \approx 1.40$.

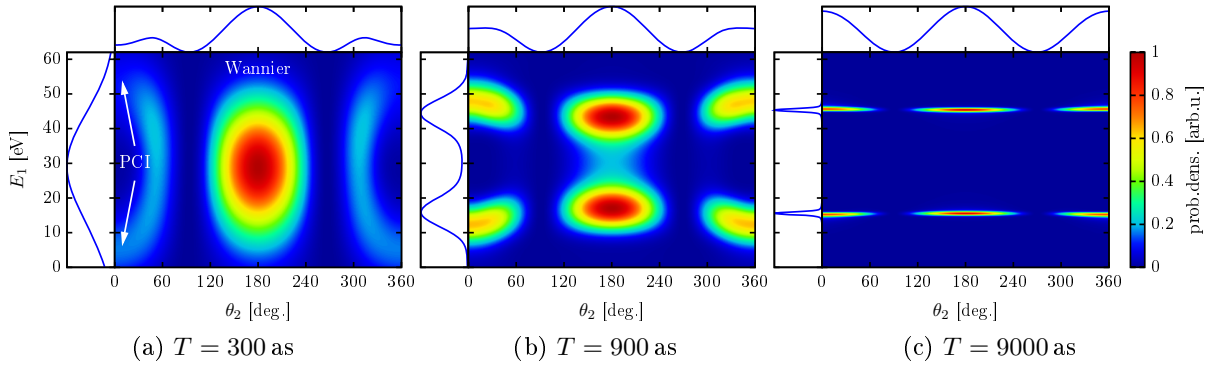


Figure 4: Angle-energy distribution $P^{DI}(E_1, \theta_1 = 0^\circ, \theta_2)$ in coplanar geometry at 70 eV photon energy for different pulse durations. The side plots show the distribution integrated over, respectively, energy and angle.

closely related to the concept of information entropy (or Shannon entropy). **Figure 3** shows that the mutual information, negligible in long pulses, strongly increases as the pulse duration is decreased. Furthermore, the pulse duration dependence of the mutual information follows a power law, $\mathcal{I}_{\Omega_1, \Omega_2} \propto 1/T^b$, with $b \approx 1.40$. The reason for this power law dependence as well as the significance of the exponent are still under investigation.

Additional insights can be gained from a projection of the two-electron momentum onto the energy-angle plane,

$$P^{DI}(E_1, \theta_{12}, \theta_1 = 0^\circ) = \int P^{DI}(E_1, E_2, \Omega_1, \Omega_2) dE_2, \quad (4)$$

in coplanar geometry and for $\theta_1 = 0^\circ$. While for long pulses the energies of the emitted electrons are independent of the relative emission angle (**Figure 4c**), strong energy-angle correlations appear for short ($T \leq 900$ as) pulses. The dominant emission channel is the back-to-back emission at equal energy sharing ($E_1 \approx 30$ eV). This corresponds precisely to the Wannier ridge riding mode [44], previously observed in e-2e ionization processes [46] and also invoked in the classification of doubly-excited resonances [47]. Because of the large instability of the Wannier orbit, its presence is more prevalent in break-up processes than in quasi-bound resonances. A second subdominant but equally interesting channel opens for short pulses at $\theta_{12} = 0^\circ$, i.e. emission in the *same*

direction. One of the electrons is slowed down while the other one is accelerated. Hence, the slow electron “pushes” the fast electron from behind, transferring part of the energy absorbed from the photon field to the faster electron. This is the well-known *post-collision interaction* [48–50] first observed by Barker and Berry in the decay of autoionizing states excited through ion impact [51].

4. Shake-up interferences

We now turn to the additional structures at higher ($E \approx \hbar\omega - I_2 + \mathcal{E}_2$) and lower ($E \approx \hbar\omega - I_1 - \mathcal{E}_2$) energies in the one-electron energy distribution $P^{DI}(E)$ (cf. **Figure 1**), which are discussed in more detail in [41]. They correspond to the case when the He^+ ion is left in an excited state after the absorption of the first photon, which can serve as an intermediate state in sequential TPDI. The free electron then obtains an energy of $E'_1 = \hbar\omega - I_1 - \mathcal{E}_n$ (with \mathcal{E}_n the excitation energy to the n -th shell of He^+). In the long-pulse limit, this simply leads to the appearance of shake-up satellite lines at energies E'_1 and $E'_2 = \hbar\omega - I_2 + \mathcal{E}_n$ in the one-electron energy spectrum. For ultrashort pulses, however, the nonsequential (or direct) double ionization channel becomes available as well and can lead to the same final states, creating an interference pattern. This bears some resemblance to the well-known exchange interference between e.g. photo-electrons and Auger electrons [52–55]. There is, however, a fundamental difference: while the exchange interference is intrinsically controlled by atomic parameters, namely the energy and lifetime (width) of the Auger electron, the novel interference observed here is truly a dynamical effect present only for short pulses and can be controlled by the pulse duration T .

As the dependence of the yield on the pulse duration is different for the different channels (proportional to T for the nonsequential channel, proportional to T^2 in the sequential channel), the observed spectrum strongly changes with pulse duration. For short pulses ($T < 1000$ as, cf. **Figure 1**), the yield is completely dominated by the nonsequential channel without any trace of a shake-up interference. As the pulse duration is increased, the sequential channel with shake-up becomes increasingly important. As expected from the interference of a relatively sharp peak with a smooth background, the peak resembles a Fano lineshape [56]. Thus, the position of the maximum is shifted from the position expected in the limit of infinitely long pulses. Even for relatively long pulses ($T = 9$ fs), similar to those produced in X-ray free-electron lasers, the position of the shake-up peak in the one-electron energy spectrum $P^{DI}(E)$ is shifted by a considerable fraction of an eV.

Such effects could possibly be observed in XFEL pulses, which reach focused intensities of up to 10^{16} W/cm². To confirm that the results shown here (calculated for 10^{12} W/cm²) also apply for these high intensities, we performed an additional calculation at a peak intensity of $I_0 = 5 \cdot 10^{15}$ W/cm² with a pulse duration of $T = 9$ fs. The shape of the differential yield $P^{DI}(E)$ (not shown) is almost unchanged compared to the result at 10^{12} W/cm² peak intensity, even though the ground state survival probability is only 20%. The total double ionization probability is $P^{DI} = 36\%$, i.e. more than a third of the helium atoms in the laser focus are doubly ionized. Even though the yield in the shake-up peak is only 0.6% of the total yield for that duration, this could be seen in experiment as only the integrated one-electron energy spectrum has to be observed. Moreover, from the position, strength and asymmetry of the interference peaks, information on the poorly known pulse duration of XFEL pulse “bursts” could possibly be deduced.

5. Summary

In conclusion, we have shown that attosecond XUV pulses can be used to probe, induce, and control electron correlation in two-photon double ionization. In such pulses, the scenario for “sequential” two-photon double ionization breaks down. Due to the small time interval between the two photoabsorption processes dynamical electron-electron correlations can be tuned by the

pulse duration T . The angular and angle-energy distributions reveal the signatures of electronic correlation induced by the Coulomb interaction. For short pulses, two well-known scenarios, the Wannier ridge riding mode and the post-collision interaction process, are simultaneously present in the two-electron emission spectrum.

The nonsequential channel without shake-up and the sequential shake-up channel, where the intermediate state after one-photon absorption is an excited state of the He^+ ion, can interfere. In attosecond pulses, only the channel without shake-up contributes, while in long pulses (longer than the 9 fs used here), the sequential shake-up channel dominates. For pulse durations of a few femtoseconds, the two channels are similarly important, such that interference can be clearly observed. This interference may open up the possibility to measure the duration of ultrashort XUV pulses in the femtosecond regime.

J.F., R.P., S.N., E.P., and J.B. acknowledge support by the FWF-Austria, grants No. FWF-SFB016 and FWF-P21141-N16. This research was supported in part by the NSF through TeraGrid resources provided by IU, LONI, NCSA, and TACC under grant TG-PHY090031. Additional computational time was provided under Institutional Computing at Los Alamos. The Los Alamos National Laboratory is operated by Los Alamos National Security, LLC for the National Nuclear Security Administration of the U.S. Department of Energy under Contract No. DE-AC52-06NA25396.

References

- [1] Hentschel M, Kienberger R, Spielmann C, Reider G A *et al.* 2001 *Nature* **414** 509
- [2] Sansone G, Benedetti E, Calegari F, Vozzi C *et al.* 2006 *Science* **314** 443
- [3] Goulielmakis E, Schultze M, Hofstetter M, Yakovlev V S *et al.* 2008 *Science* **320** 1614
- [4] Ackermann W, Asova G, Ayvazyan V, Azima A *et al.* 2007 *Nat. Photonics* **1** 336
- [5] Nabekawa Y, Hasegawa H, Takahashi E J and Midorikawa K 2005 *Phys. Rev. Lett.* **94** 043001
- [6] Dromey B, Zepf M, Gopal A, Lancaster K *et al.* 2006 *Nat. Phys.* **2** 456
- [7] Naumova N M, Nees J A, Sokolov I V, Hou B and Mourou G A 2004 *Phys. Rev. Lett.* **92** 063902
- [8] Seres J, Yakovlev V S, Seres E, Streltsov C, Wobrauschek P, Spielmann C and Krausz F 2007 *Nat. Phys.* **3** 878
- [9] Zhang X, Lytle A L, Popmintchev T, Zhou X, Kapteyn H C, Murnane M M and Cohen O 2007 *Nat. Phys.* **3** 270
- [10] Nomura Y, Horlein R, Tzallas P, Dromey B *et al.* 2009 *Nat. Phys.* **5** 124
- [11] Parker J S, Smyth E S and Taylor K T 1998 *J. Phys. B* **31** L571
- [12] Byron F W and Joachain C J 1967 *Phys. Rev.* **164** 1
- [13] Proulx D and Shakeshaft R 1993 *Phys. Rev. A* **48** R875
- [14] Bräuning H, Dörner R, Cocke C L, Prior M H *et al.* 1998 *J. Phys. B* **31** 5149
- [15] Briggs J S and Schmidt V 2000 *J. Phys. B* **33** R1
- [16] Malegat L, Selles P and Kazansky A K 2000 *Phys. Rev. Lett.* **85** 4450
- [17] Lein M, Gross E K U and Engel V 2000 *Phys. Rev. Lett.* **85** 4707
- [18] Staudte A, Ruiz C, Schöffler M, Schössler S *et al.* 2007 *Phys. Rev. Lett.* **99** 263002
- [19] Rudenko A, de Jesus V L B, Ergler T, Zrost K *et al.* 2007 *Phys. Rev. Lett.* **99** 263003
- [20] Nikolopoulos L A A and Lambropoulos P 2001 *J. Phys. B* **34** 545
- [21] Colgan J and Pindzola M S 2002 *Phys. Rev. Lett.* **88** 173002

- [22] Feng L and van der Hart H W 2003 *J. Phys. B* **36** L1
- [23] Hu S X, Colgan J and Collins L A 2005 *J. Phys. B* **38** L35
- [24] Fomouo E, Lagmago Kamta G, Edah G and Piraux B 2006 *Phys. Rev. A* **74** 063409
- [25] Ivanov I A and Kheifets A S 2007 *Phys. Rev. A* **75** 033411
- [26] Nikolopoulos L A A and Lambropoulos P 2007 *J. Phys. B* **40** 1347
- [27] Pronin E A, Manakov N L, Marmo S I and Starace A F 2007 *J. Phys. B* **40** 3115
- [28] Horner D A, McCurdy C W and Rescigno T N 2008 *Phys. Rev. A* **78** 043416
- [29] Feist J, Nagele S, Pazourek R, Persson E, Schneider B I, Collins L A and Burgdörfer J 2008 *Phys. Rev. A* **77** 043420
- [30] Antoine P, Fomouo E, Piraux B, Shimizu T, Hasegawa H, Nabekawa Y and Midorikawa K 2008 *Phys. Rev. A* **78** 023415
- [31] Guan X, Bartschat K and Schneider B I 2008 *Phys. Rev. A* **77** 043421
- [32] Hasegawa H, Takahashi E J, Nabekawa Y, Ishikawa K L and Midorikawa K 2005 *Phys. Rev. A* **71** 023407
- [33] Sorokin A A, Wellhofer M, Bobashev S V, Tiedtke K and Richter M 2007 *Phys. Rev. A* **75** 051402(R)
- [34] Laulan S and Bachau H 2003 *Phys. Rev. A* **68** 013409
- [35] Piraux B, Bauer J, Laulan S and Bachau H 2003 *Eur. Phys. J. D* **26** 7
- [36] Ishikawa K L and Midorikawa K 2005 *Phys. Rev. A* **72** 013407
- [37] Barna I F, Wang J and Burgdörfer J 2006 *Phys. Rev. A* **73** 023402
- [38] Horner D A, Morales F, Rescigno T N, Martín F and McCurdy C W 2007 *Phys. Rev. A* **76** 030701(R)
- [39] Fomouo E, Antoine P, Bachau H and Piraux B 2008 *New J. Phys.* **10** 025017
- [40] Palacios A, Rescigno T N and McCurdy C W 2009 *Phys. Rev. A* **79** 033402
- [41] Feist J, Pazourek R, Nagele S, Persson E, Schneider B I, Collins L A and Burgdörfer J 2009 *J. Phys. B* **42** 134014
- [42] Feist J, Nagele S, Pazourek R, Persson E, Schneider B I, Collins L A and Burgdörfer J 2009 *Phys. Rev. Lett.* **103** 063002
- [43] Ullrich J, Moshhammer R, Dorn A, Dörner R, Schmidt L P H and Schmidt-Böcking H 2003 *Rep. Prog. Phys.* **66** 1463
- [44] Wannier G H 1953 *Phys. Rev.* **90** 817
- [45] Gray R M 1990 *Entropy and Information Theory* (Springer) 1 edn.
- [46] Cvejanovic S and Read F H 1974 *J. Phys. B* **7** 1841
- [47] Tanner G, Richter K and Rost J M 2000 *Rev. Mod. Phys.* **72** 497
- [48] Gerber G, Morgenstern R and Niehaus A 1972 *J. Phys. B* **5** 1396
- [49] Russek A and Mehlhorn W 1986 *J. Phys. B* **19** 911
- [50] Armen G B, Tulkki J, Åberg T and Crasemann B 1987 *Phys. Rev. A* **36** 5606
- [51] Barker R B and Berry H W 1966 *Phys. Rev.* **151** 14
- [52] Végh L and Macek J H 1994 *Phys. Rev. A* **50** 4031
- [53] Read F H 1977 *J. Phys. B* **10** L207
- [54] de Gouw J A, van Eck J, Peters A C, van der Weg J and Heideman H G M 1993 *Phys. Rev. Lett.* **71** 2875
- [55] Rouvellou B, Rioual S, Avaldi L, Camilloni R, Stefani G and Turri G 2003 *Phys. Rev. A* **67** 012706
- [56] Fano U 1961 *Phys. Rev.* **124** 1866